

ANNA JASIK

ORCID: 0000-0001-7413-486X

Silesian University of Technology, Department of Materials Technology, Material Innovation Laboratory, Katowice, Poland

DOI: 10.15199/40.2023.9.2

# Numerical simulations of temperature and stress distribution in thermal barrier coatings in the context of differences in input data values – bond coat and substrate materials

## Symulacje numeryczne rozkładu temperatury oraz stanu naprężen w powłokowych barierach cieplnych w kontekście różnic w wartościach danych wejściowych – warstwa pośrednia i materiał podłoża

The article presents the research results on the impact of differences in input data values concerning materials used in thermal barrier coating systems on the results of the finite element method (FEM) simulation of temperature distribution and Huber-Mises equivalent stresses. This article focuses on the material parameters characterizing the intermediate layer and the base material. It was shown that, as in the case of the 8YSZ ceramic layer, the data are characterized by a very wide scatter of values. It was found that the results of the simulations obtained with the use of these data differ significantly from each other, depending on the adopted reference point, i.e. whether minimum, maximum, median or average values were adopted for the simulation. Therefore, considering the total differences in simulations resulting from the scattering of input data for the substrate material, interlayer and ceramic layer, it should be stated that it is possible to obtain virtually any simulation result.

**Keywords:** FEM, TBC, simulations, input data, reliability of calculations

### 1. Introduction

The credibility of input data in numerical simulations, e.g. carried out using the finite element method, determines the correctness and reliability of the final results obtained. Introducing incorrect data or data from unreliable and undocumented sources may cause errors in the analyses carried out and threaten the operation of structures, components or other systems operating in specific temperatures, stress and environmental conditions. This problem also concerns shell thermal barriers (TBC), an important element of stationary and non-stationary gas turbines, e.g. aircraft engines [1].

W artykule przedstawiono wyniki badań nad wpływem różnic w wartościach danych wejściowych dotyczących materiałów używanych w systemach powłokowych barier cieplnych na wyniki symulacji metodą elementów skończonych (MES) rozkładu temperatury i naprężen zastępczych Hubera-Misesa. Skupiono się na parametrach materiałowych charakteryzujących warstwę pośrednią oraz materiał podłożowy. Wykazano, że tak jak w przypadku warstwy ceramicznej 8YSZ dane charakteryzują się bardzo szerokim rozrzutem wartości. Stwierdzono, że wyniki symulacji z użyciem tych danych różnią się znacznie od siebie w zależności od przyjętego punktu odniesienia, to znaczy od tego, czy do symulacji przyjęto wartości minimalne, maksymalne, medianę czy średnią. Uwzględniając zatem sumaryczne różnice w symulacjach wynikające z rozrzutu danych wejściowych dla materiału podłożu, międzywarstwy oraz warstwy ceramicznej, należy stwierdzić, że możliwe jest uzyskanie praktycznie dowolnego wyniku symulacji.

**Słowa kluczowe:** MES, TBC, symulacje, dane wejściowe, wiarygodność obliczeń

TBC systems are used in gas turbines and their role is to protect the metallic substrate of the combustion chambers or stationary blades from extremely high temperatures. They are extremely effective thermal insulation based on the thermal properties of the materials used for their production (ceramics with ultra-low thermal conductivity) and advanced internal cooling methods [1]. The effectiveness of TBC systems in the operating conditions of gas turbines is determined by their durability, which depends on the operating conditions (high temperature, complex state of stress, aggressive working environment). These factors make TBC systems vulnerable to cracking of the ceramic layer and its detachment [2–4]. Predicting the durability of TBC systems is one of the

**Anna Jasik, BEng, PhD** – is an assistant professor in the Faculty of Materials Engineering of the Silesian University of Technology in Gliwice. In 1999 she graduated from the Faculty of Engineering and Metallurgy at the Silesian University of Technology. Then, in 1999–2005, she was a PhD student in Materials Engineering and Metallurgy. Her scientific interests primarily focused on issues related to biomechanical problems. At the current time, her basic area of scientific interest is connected to FEM simulations of coatings systems, especially thermal barrier coatings used in aircraft and stationary gas turbines. She is the author and co-author of many scientific publications in this area published in recognized journals of national and international range. Currently, she is working on the problem of the analytical model of microstructure, which can be used for FEM simulations of TBC systems, which will ensure the possibility of performing reliable FEM calculations based on DFT source data.

E-mail: anna.jasik@polsl.pl

■ Otrzymano / Received: 10.08.2023. Przyjęto / Accepted: 04.09.2023

most important aspects of their design. However, as mentioned earlier, the critical factor in the correct simulation calculation process is the correctness of the entered input data. A wide range of material data for the same material (interlayer and substrate) is available in literature sources but with significantly different values, which makes simulations worthless. As mentioned in the article [5], a perfect example is the material data for the basic material used in thermal barriers, i.e. zirconium oxide modified with yttrium oxide (8YSZ: 8%  $\text{Y}_2\text{O}_3 \times \text{ZrO}_2$  in at%). This article, which is a continuation of the analysis from the publication [5], presents the results of research on the influence of the dispersion of input material data on the NiCrAlY interlayer and the nickel-based superalloy used in numerical modelling of temperature distribution and state of stress in thermal barrier coatings. The paper summarizes the data contained in the professional literature in the field of finite element simulation of TBC systems and

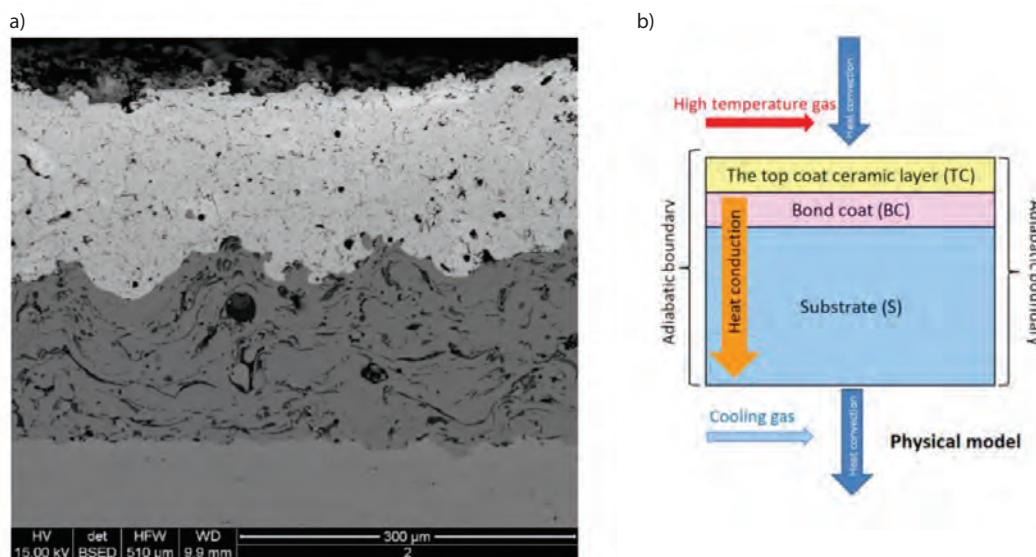


Fig. 1. Physical model of the TBC system: a) actual microstructure, b) schematic structure of the model with ceramic coating  
Rys. 1. Model fizyczny systemu TBC: a) mikrostruktura, b) schemat modelu z powłoką ceramiczną

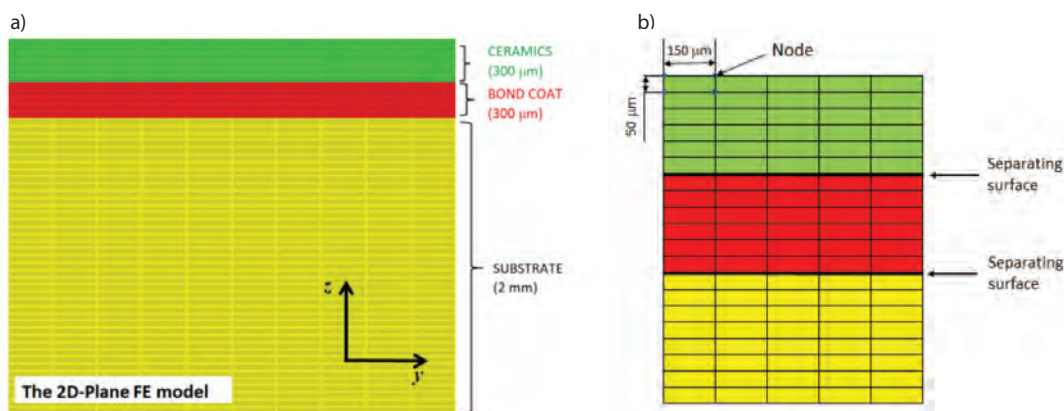


Fig. 2. Discrete model of the TBC system: a) fragment of the finite element mesh of the model, b) ceramic coating with a typical finite element mesh  
Rys. 2. Model dyskretny systemu TBC: a) fragment siatki elementów skończonych modelu, b) powłoka ceramiczna z typową siatką elementów skończonych

**Table 1. Set of material data used in FEM simulations**

**Tabela 1. Zestaw danych materiałowych użytych w symulacjach MES**

| Material                          | Properties                  | Values of material properties |                        |                       |                        |                        |                        |                        |
|-----------------------------------|-----------------------------|-------------------------------|------------------------|-----------------------|------------------------|------------------------|------------------------|------------------------|
|                                   |                             | min.                          | max.                   | st. dev.              | average                | median                 | kurtosis               | skewness               |
| 8YSZ – top ceramic coat           | $\lambda$ [W/mK]            | 0.90                          | 2.17                   | 0.46                  | 1.49                   | 1.10                   | -1.97                  | 0.40                   |
|                                   | $c_p$ [J/kgK]               | 0.405                         | 0.656                  | 0.085                 | 0.502                  | 0.500                  | 2.62                   | 1.25                   |
|                                   | CTE [1/K]                   | $8.20 \times 10^{-6}$         | $12.20 \times 10^{-6}$ | $0.92 \times 10^{-6}$ | $9.52 \times 10^{-6}$  | $9.68 \times 10^{-6}$  | $3.43 \times 10^{-6}$  | $1.14 \times 10^{-6}$  |
|                                   | $E$ [GPa]                   | 17.5                          | 210.0                  | 60.7                  | 74.7                   | 48.0                   | 1.69                   | 1.66                   |
|                                   | $v$                         | 0.10                          | 0.26                   | 0.06                  | 0.19                   | 0.20                   | -1.63                  | -0.36                  |
|                                   | $\rho$ [kg/m <sup>3</sup> ] | 5.40                          | 6.04                   | 0.27                  | 5.76                   | 5.60                   | 3.58                   | -1.85                  |
| MeCrAlY (Me = Ni, Co) – bond coat | $\lambda$ [W/mK]            | 4.30                          | 25.00                  | 8.16                  | 11.6                   | 11.2                   | 2.23                   | 1.41                   |
|                                   | $c_p$ [J/kgK]               | 0.40                          | 0.501                  | 0.06                  | 0.5                    | 0.5                    | –                      | -1.73                  |
|                                   | CTE [1/K]                   | $11.60 \times 10^{-6}$        | $15.50 \times 10^{-6}$ | $1.50 \times 10^{-6}$ | $13.6 \times 10^{-6}$  | $13.3 \times 10^{-6}$  | $-1.89 \times 10^{-6}$ | $0.07 \times 10^{-6}$  |
|                                   | $E$ [GPa]                   | 137.90                        | 225.00                 | 25.47                 | 188.3                  | 200.0                  | 0.30                   | -0.89                  |
|                                   | $v$                         | 0.27                          | 0.32                   | 0.01                  | 0.3                    | 0.3                    | 4.00                   | -1.25                  |
|                                   | $\rho$ [kg/m <sup>3</sup> ] | 7.32                          | 7.80                   | 0.34                  | 7.6                    | 7.6                    | –                      | –                      |
| Ni-based superalloys – substrate  | $\lambda$ [W/mK]            | 7.00                          | 90.00                  | 35.73                 | 38.25                  | 12.53                  | -2.02                  | 0.69                   |
|                                   | $c_p$ [J/kgK]               | 0.41                          | 0.48                   | 0.03                  | 0.44                   | 0.45                   | -1.17                  | -0.32                  |
|                                   | CTE [1/K]                   | $9.67 \times 10^{-6}$         | $16.40 \times 10^{-6}$ | $1.78 \times 10^{-6}$ | $12.91 \times 10^{-6}$ | $13.10 \times 10^{-6}$ | $0.22 \times 10^{-6}$  | $-0.09 \times 10^{-6}$ |
|                                   | $E$ [GPa]                   | 15.00                         | 220.00                 | 52.97                 | 177.29                 | 200.50                 | 5.69                   | -2.23                  |
|                                   | $v$                         | 0.25                          | 0.32                   | 0.02                  | 0.30                   | 0.30                   | 0.99                   | -1.35                  |
|                                   | $\rho$ [kg/m <sup>3</sup> ] | 7.9                           | 8.9                    | 3.97                  | 8.42                   | 8.23                   | -2.44                  | 0.18                   |

Source: the author, based on [3, 5–7, 9, 10–65].

Źródło: opracowanie własne na podstawie [3, 5–7, 9, 10–65].

concerning material data. For the purposes of this article, only the minimum and maximum values and the standard deviation of the results, as well as the mean and median values, are presented.

## 2. Experiment procedure

TBC numerical models allow you to simulate the behaviour of systems, such as thermal barriers when operating under real conditions, which helps in the analysis and optimization of the system. Discrete models are particularly useful because they allow individual layers of finite elements to be evenly distributed, translating into more accurate results. An important aspect of the analysis of TBC models is the consideration of the thermo-mechanical properties of materials (such as coefficients of thermal expansion, strength, modulus of elasticity, etc.), thermal and mechanical interactions between the layers, and evaluation of the behaviour of the TBC under operating conditions.

The procedure for finite element modelling with the main steps is presented below:

1. Definition of the model's geometry: an axisymmetric two-dimensional model.
2. Division of geometry into finite elements (discretization of elements that form the whole model).
3. Determining the boundary conditions that correspond to the real conditions of the model operation. Temperature load assignment.
4. Determination of material properties: Young's modulus, Poisson's ratio, thermal expansion coefficient, thermal conductivity, etc.
5. Formulation of equations: based on physical and mathematical equations, such as equilibrium equations, heat equations, etc., appropriate equations were formulated describing the behaviour of the material and its response to defined boundary conditions.
6. Performing a numerical analysis by solving a system of equations for all finite elements in the model. The result of the calculations will be the distribution of temperature, stresses and strains in the entire model.

Based on the real picture of the microstructure of TBC systems, a discrete model of thermal barriers was developed, shown in Fig. 1. The geometric model includes three layers: a base made of IN 625 nickel superalloy with a thickness of 2 mm, an intermediate layer (interlayer) made of Amdry 962 alloy (Ni-22Cr-10Al-1Y in at%) with a thickness of 300 µm and an insulating ceramic coating of the Metco 204NS type (8YSZ:  $8\text{Y}_2\text{O}_3 \times \text{ZrO}_2$  in at%), also with a thickness of 300 µm. In the case of simple geometric elements used in the model, as shown in Fig. 2a, the 2D discrete model allows for the even distribution of individual layers of finite elements. Each layer corresponds to the corresponding material, i.e. the substrate, the interlayer and the ceramic layer. The number of rows of individual finite elements allows for any control of the thickness of each layer of the analysed TBC system. Figure 2b shows the analysed TBC system's discrete internal structure and geometry. Due to simplifying the calculation procedure, an axisymmetric character of the assumed stresses was proposed. In the analysed problem, 2D axisymmetric, four-node elements were adopted.

The following assumptions were taken into account for the analysis of the temperature field and stress state at high temperatures:

- all layers are homogeneous and isotropic;
- the left and right sides of the model are treated as adiabatic boundaries, where there is no heat exchange with the environment;

- the temperature near the ceramic layer was assumed to be 1500°C (flue gas temperature), while the surface temperature was 800°C (cooling air temperature).

The tests include the analysis of elastic deformations. Two variants of the calculation procedure were adopted in the numerical analysis. In the first one, the following assumptions were made: the material properties of the ceramic layer were taken as their median, the physical properties of the base material were taken based on the IN 625 alloy manufacturer's data [6]. The interlayer was characterized by the following values of material properties: minimum value, maximum value, average value and corresponding to the median. In the second variant, the median values of material parameters for ceramics and the interlayer were assumed as the output parameters. In contrast, the properties of the substrate material (IN 625) were assumed in the form of values corresponding to minimum, maximum, average and median. The first stage of the research was to conduct a numerical analysis of the temperature field. The conditions of heat transfer on the outer surfaces of the body were determined by applying the boundary conditions of the first kind. The solution to the problem consisted in determining the temperature distribution based on the considered body's given initial and boundary conditions and material properties. In the analysed model, a temperature load was assumed. The temperature of 1500°C was set on the surface of the insulating ceramic layer of the TBC system, while the temperature of 800°C was assumed on the outer surface of the nickel superalloy. The next research stage was to determine the distribution of equivalent stresses following the Huber-Mises hypothesis for all variants of the assumptions of material values. The material data set in Table 1 was used for the FEM analysis. It includes the maximum and minimum values of the parameters (derived from literature data) as well as the mean value and the median (and other statistical parameters) determined for the purposes of this article. To illustrate the dispersion of the data, the standard deviation for each parameter was also introduced.

## 3. Results

As in the case of the YSZ-type material [5], the first stage of the research was the analysis of source data characterizing the basic physical parameters of the materials used in the simulations. This part discusses the data on the interlayer and substrate materials – NiCrAlY-type alloys and nickel-based superalloys.

Data on the material properties of the NiCrAlY interlayer show a large dispersion, especially in thermal conductivity and, to some extent, Young's modulus. The remaining parameters show a small dispersion of results, which is also expressed by statistical parameters. Due to the relatively small amount of data, we failed in all cases of kurtosis and skewness.

The situation is slightly different in the case of the base material in the form of a nickel superalloy. The spread of data in this case is comparable to the material dedicated to the insulating layer, i.e. YSZ. This applies to the thermal conductivity value, coefficient of thermal expansion and Young's modulus.

The analysis of the source data in the case of the ceramic material 8YSZ [5] indicated the reason for the differences in the data values characterizing the physical properties of the materials used in FEM simulations. There are differences in the morphology and form of material processing. On the other hand, in the case of NiCrAlY-type superalloys, there are quite limited morphological differences. The main data concerned the NiCrAlY material in thermally sprayed coatings. Hence, the scatter of results is smaller than in the case of ceramic material

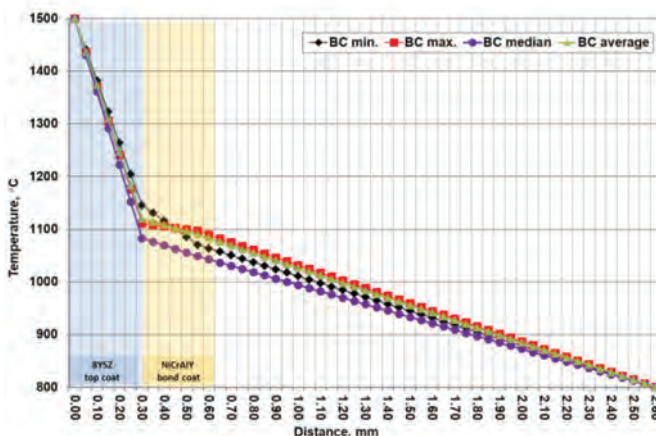
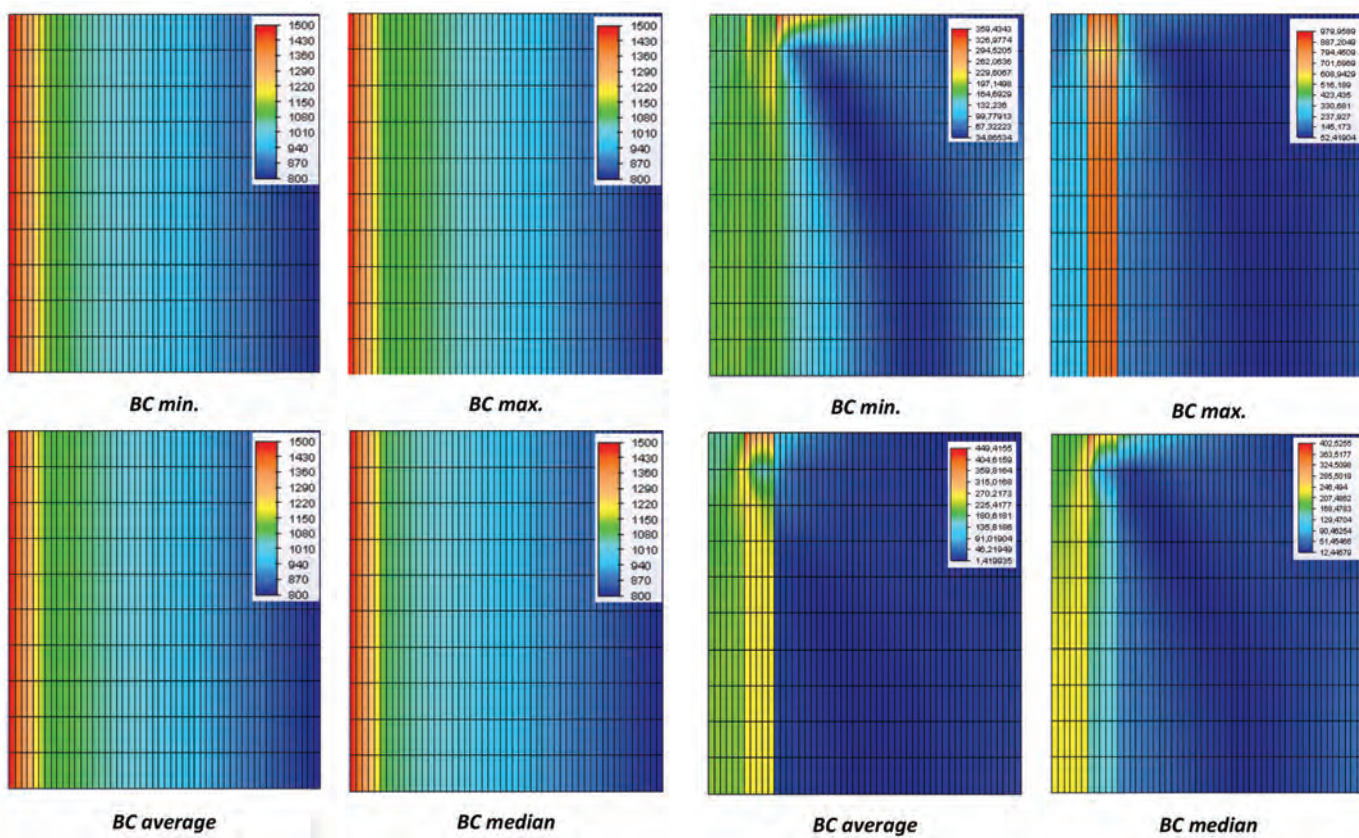


Fig. 3. The results of the simulation of temperature distribution for different values (minimum, maximum, median, average) of physical parameters of materials – bond coat

Rys. 3. Wyniki symulacji rozkładu temperatury dla różnych wartości (minimum, maksimum, mediany, średniej) parametrów fizycznych materiałów – międzywarstwa

8YSZ. The situation is different in the case of the base material where the literature data often lacks information on the type of superalloy used. There are also simulations in which pure nickel was introduced as the base material, the thermal conductivity of which is many times greater than the thermal conductivity of any nickel superalloy. Hence, significantly greater differences in the simulation results are considered from the point of view of the input data for the substrate material compared to the analogous results for the interlayer.

Figures 3–6 show the temperature and stress distribution simulation results. Obtained based on the data contained in Table 1,

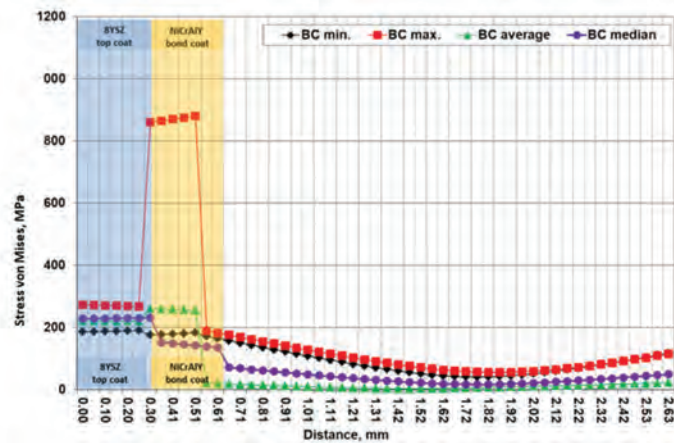


Fig. 4. Results of simulation of von Mises stress distribution for different values of physical parameters of materials: for a constant temperature of 1200°C – bond coat

Rys. 4. Wyniki symulacji rozkładu naprężzeń według hipotezy Hubera-Misesa dla różnych wartości parametrów fizycznych materiałów: dla stałej temperatury 1200°C – międzywarstwa

i.e. minimum values, maximum, median and average of the basic parameters characterizing the physical properties of materials necessary in the FEM modelling process.

Similarly to the YSZ [5], the analyses showed that introducing extreme values results in obtaining simulation results significantly different in temperature distribution. Considering the effect of the interlayer, it should be noted that if minimum values are entered, the temperature on the surface of the interlayer differs by as much as approx. 25°C compared to the maximum values and 65°C to the median. Considering the influence of the substrate material these differences are much greater and

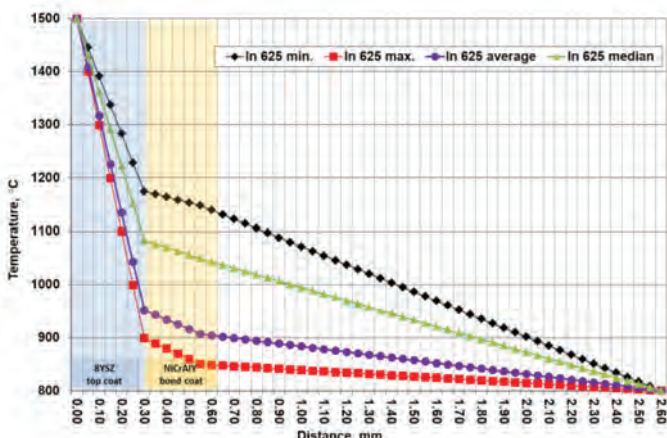
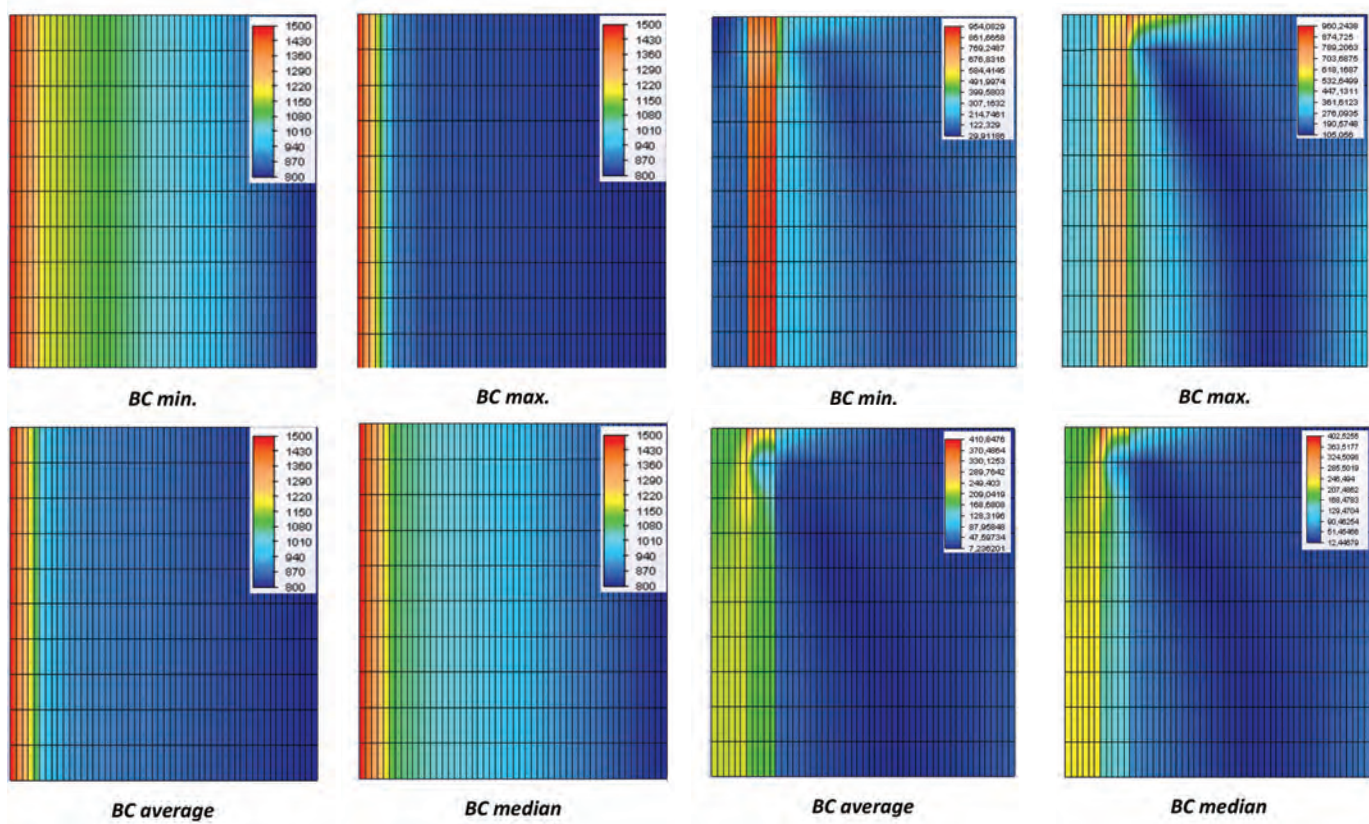


Fig. 5. The results of the simulation of the temperature distribution for different values (minimum, maximum, median, average) of the physical parameters of the materials – the substrate

Rys. 5. Wyniki symulacji rozkładu temperatury dla różnych wartości (minimum, maksimum, mediany, średniej) parametrów fizycznych materiałów – podłoże

amount to approx. 275°C for the minimum and maximum extreme values.

In the case of the bond coat, it is difficult to talk about a trend when entering the minimum, maximum, mean or median values, which is quite an unusual observation. On the other hand, in the case of the substrate material, for the median, the temperature on the surface of the interlayer is close to that obtained for the minimum value and the average value to the maximum value.

In the case of reduced stresses (for the interlayer), the strongest gradient effect was obtained for maximum values. In the remaining cases, the differences in stress at the separation boundaries

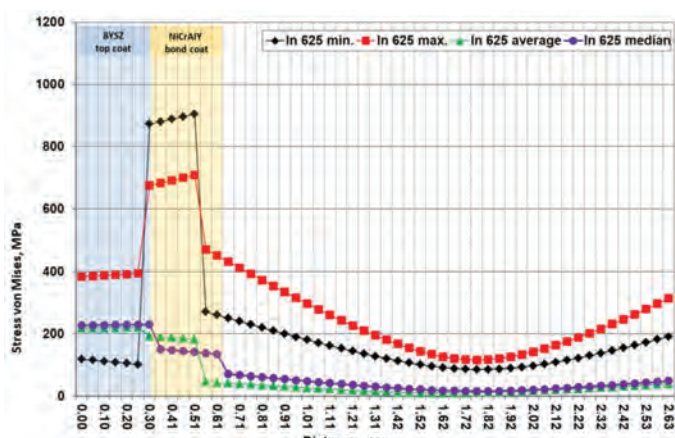


Fig. 6. Results of simulation of von Mises stress distribution for different values of physical parameters of materials: for a constant temperature of 1200°C – substrate

Rys. 6. Wyniki symulacji rozkładu naprężen zastępczych według hipotezy Hubera-Misesa dla różnych wartości parametrów fizycznych materiałów: dla stałej temperatury 1200°C – podłoże

of individual sublayers are very similar. When considering the variant concerning the base material, the most favourable stress distribution can be observed after introducing the median or the average as input parameters for the FEM simulation.

#### 4. Conclusions

The analyses carried out in the form of FEM simulations, regarding the interlayer's influence on the distribution of temperature and stresses showed that significant differences are observed in the case of reduced von Mises stresses (for the

maximum and minimum values). In the case of temperature distribution, the differences are relatively small. However, an unusual relationship is visible when the median or mean value is entered. In this case, the temperature distribution is not located between the maximum and minimum values. This suggests that other factors besides thermal conductivity also affect the temperature distribution.

In the case of simulations based on data on the physical properties of the base material (nickel superalloys), a large scatter of input data causes significant differences in the results of simulations of temperature distribution and reduced stresses. In the context of the scattering of input data, the observed differences in simulation results are obvious.

These data also show that the most favourable substrate material, from the point of view of temperature distribution, is a nickel superalloy with the highest possible thermal conductivity value. The most favourable state of stress was observed for the mean and median values of the introduced physical properties of the base material.

### Acknowledgements

The work was carried out under the statutory subsidy of the Silesian University of Technology at the Faculty of Materials Engineering (11/030/BK\_23/1127).

### BIBLIOGRAPHY

- [1] N. P. Padture, M. Gell, E. H. Jordan. 2002. "Thermal Barrier Coatings for Gas-Turbine Engine Applications." *Science* 296(5566): 280–284. DOI: 10.1126/science.1068609.
- [2] H. E. Evans. 2011. "Oxidation Failure of TBC Systems: An Assessment of Mechanisms." *Surface and Coatings Technology* 206(7): 1512–1521. DOI: 10.1016/j.surcoat.2011.05.053.
- [3] M. Białas. 2008. "Finite Element Analysis of Stress Distribution in Thermal Barrier Coatings." *Surface and Coatings Technology* 202(24): 6002–6010. DOI: 10.1016/j.surcoat.2008.06.178.
- [4] E. P. Busso, Z. Qian, M. P. Taylor, H. E. Evans. 2009. "The Influence of Bondcoat and Topcoat Mechanical Properties on Stress Development in Thermal Barrier Coating Systems." *Acta Materialia* 57(8): 2349–2361. DOI: 10.1016/j.actamat.2009.01.017.
- [5] A. Jasik. 2023. "Numerical Simulations of Temperature and Stress Distribution in Thermal Barrier Coatings in the Context of Differences in Input Data Values – External Ceramic Layer." *Ochrona przed Korozją* 66(8): 247–252. DOI: 10.15199/40.2023.8.4.
- [6] www.specialmetals.com (access: 17.07.2023).
- [7] H. S. Zhang, H. C. Sun, X. G. Chen. 2012. "Effect of Top-Layer Thickness on Residual Stresses of Plasma-Spraying  $\text{Sm}_2\text{Zr}_2\text{O}_7/\text{YSZ}$  Thermal Barrier Coatings." *Advanced Materials Research* 347–353: 40–43. DOI: 10.4028/www.scientific.net/amr.347-353.40.
- [8] K. Slámečka, P. Skalka, J. Pokluda, L. Čelko. 2016. "Finite Element Simulation of Stresses in a Plasma-Sprayed Thermal Barrier Coating with an Irregular Top-Coat/Bond-Coat Interface." *Surface and Coatings Technology* 304: 574–583. DOI: 10.1016/j.surcoat.2016.07.066.
- [9] P. Bednarz, R. Herzog, E. Trunova, R. W. Steinbrech, H. Echsler, W. J. Quadakkers, F. Schubert, L. Singheiser. 2005. *Stress Distribution in APS-TBCs under Thermal Cycling Loading Conditions*. In: D. Zhu and K. Plucknett (eds). *Advances in Ceramic Coatings and Ceramic-Metal Systems: Ceramic Engineering and Science Proceedings*. Westerville, Ohio: The American Ceramic Society. DOI: 10.1002/9780470291238.ch9.
- [10] A. Liu, Y. Wei. 2003. "Finite Element Analysis of Anti-Spallation Thermal Barrier Coatings." *Surface and Coatings Technology* 165(2): 154–162. DOI: 10.1016/S0257-8972(02)00743-0.
- [11] M. Abbas, H. J. Hasham, Y. Baig. 2016. "Numerical Parametric Analysis of Bond Coat Thickness Effect on Residual Stresses in Zirconia-Based Thermal Barrier Coatings." *High-Temperature Materials and Processes* 35(2): 201–207. DOI: 10.1515/htmp-2014-0185.
- [12] M. Abbas, L. Guo, H. Guo. 2013. "Evaluation of Stress Distribution and Failure Mechanism in Lanthanum–Titanium–Aluminum Oxides Thermal Barrier Coatings." *Ceramics International* 39(5): 5103–5111. DOI: 10.1016/j.ceramint.2012.12.006.
- [13] M. Abbas, H. Guo, M. R. Shahid. 2013. "Comparative Study on Effect of Oxide Thickness on Stress Distribution of Traditional and Nanostructured Zirconia Coating Systems." *Ceramics International* 39(1): 475–481. DOI: 10.1016/j.ceramint.2012.06.051.
- [14] N. Nayebpashaei, E. Etemadi, B. Mohammad Sadeghi, S. H. Seydein. 2021. "Experimental and Numerical Study of the Thermo-Mechanical Behavior of Plasma-Sprayed Gadolinium and Yttria Zirconate-Based Thermal Barrier Coatings." *Advanced Ceramics Progress* 7(4): 36–51. DOI: 10.30501/acp.2022.322563.1078.
- [15] F. Yang, J. C. M. Li (eds). 2008. *Micro and Nano Mechanical Testing of Materials and Devices*. New York: Springer.
- [16] A. D. Johari, S. Mohd Yunus, S. Husin. 2020. "Comparison on Thermal Resistance Performance of YSZ and Rare-Earth GZ Multilayer Thermal Barrier Coating at 1250°C Gas Turbine Combustor Liner." *Journal of Advanced Research in Fluid Mechanics and Thermal Sciences* 52(2): 123–128.
- [17] P. Zhang, Y. Feng, Y. Li, W. Pan, P. Zong, M. Huang, Y. Han, Z. Yang, H. Chen, Q. Gong, C. Wan. 2020. "Thermal and Mechanical Properties of Ferroelastic  $\text{RENb}_4\text{O}_9$  ( $\text{RE} = \text{Nd}, \text{Sm}, \text{Gd}, \text{Dy}, \text{Er}, \text{Yb}$ ) for Thermal Barrier Coatings." *Scripta Materialia* 180: 51–56. DOI: 10.1016/j.scriptamat.2020.01.026.
- [18] C. H. Hsueh, P. F. Becher, E. R. Fuller, S. A. Langer, W. C. Carter. 1999. "Surface-Roughness Induced Residual Stresses in Thermal Barrier Coatings: Computer Simulations." *Materials Science Forum* 308–311: 442–449. DOI: 10.4028/www.scientific.net/MSF.308-311.442.
- [19] M. Ranjbar-Far, J. Absi, G. Mariaux, F. Dubois. 2010. "Simulation of the Effect of Material Properties and Interface Roughness on the Stress Distribution in Thermal Barrier Coatings Using Finite Element Method." *Materials and Design* 31(2): 772–781. DOI: 10.1016/j.matdes.2009.08.005.
- [20] K. Sfar, J. Aktaa, D. Munz. 2002. "Numerical Investigation of Residual Stress Fields and Crack Behavior in TBC Systems." *Materials Science and Engineering: A* 333(1–2): 351–360. DOI: 10.1016/S0921-5093(01)01859-7.
- [21] G. Kerkhoff, R. Vaßen, D. Stöver. 1999. *Numerically Calculated Thermal Stresses in Thermal Barrier Coatings on Cylindrical Substrates*. In: E. Lugscheider, P. A. Kammer (eds). *United Thermal Spray Conference (UTSC 1999)*. Materials Park, Ohio: ASM International.
- [22] K. Sfar, J. Aktaa, D. Munz. 2000. *Analysing the Failure Behaviour of Thermal Barrier Coatings Using the Finite Element Method*. In: T. Jessen, E. Ustundag (eds). *24th Annual Conference on Composites, Advanced Ceramics, Materials, and Structures: A: Ceramic Engineering and Science Proceedings*. Westerville, Ohio: The American Ceramic Society. DOI: 10.1002/9780470294628.ch23.
- [23] H. Zimmermann. 1992. *Elastische Eigenschaften verschiedener keramischer Materialien*. Kernforschungszentrum Karlsruhe: KfK 5092.
- [24] H. Zimmermann. 1994. *Thermoschock- und Temperaturwechselverhalten verschiedener keramischer Materialien*. Kernforschungszentrum Karlsruhe: KfK 5303.
- [25] R. Kowalewski. 1997. *Thermomechanische Ermüdung einer beschichteten, stengelkristallinen Nickelbasis-Superlegierung*. Düsseldorf: VDI Verlag.
- [26] W. Mannsmann. 1995. *Keramische Wärmedämmsschichtsysteme: Eigenschaften und Verhalten unter mechanischer, thermischer und thermomechanischer Beanspruchung*. PhD thesis. Karlsruhe: Fakultät für Maschinenbau der Universität Karlsruhe.
- [27] M. Alaya. 1997. *Bewertung und Optimierung von Konzepten zur Verbesserung des Einsatzverhaltens von  $\text{ZrO}_2$ -Wärmedämmsschichtsystemen*. PhD thesis. Karlsruhe: Fakultät für Maschinenbau der Universität Karlsruhe.
- [28] A. Burov, E. Fedorova. 2020. "Modeling of Interface Failure in a Thermal Barrier Coating System on Ni-Based Superalloys." *Engineering Failure Analysis* 123: 105320. DOI: 10.1016/j.engfailanal.2021.105320.
- [29] J. Cheng, E. H. Jordan, B. Barber, M. Gell. 1998. "Thermal/Residual Stress in an Electron Beam Physical Vapor Deposited Thermal Barrier Coating System." *Acta Materialia* 46(16): 5839–5850. DOI: 10.1016/S1359-6454(98)00230-4.
- [30] J. B. Wachtman, W. R. Cannon, M. Matthewson. 1996. *Mechanical Properties of Ceramics*. New York: John Wiley and Sons.
- [31] R. V. Hillery, B. H. Pilisner, R. L. McKnight, T. S. Cook, M. S. Hartle. 1988. *Thermal Barrier Coating Life Prediction Model Development: Final Report*. NASA Contract Report 180807.
- [32] G. Simmons, H. Wang. 1971. *Single Crystal Elastic Constants and Calculated Aggregate Properties: A Handbook*. Cambridge, Massachusetts: MIT Press.
- [33] E. A. Brandes, G. B. Brook (eds). 1983. *Smithells Metals Reference Book*. London: Butterworth.

- [34] R. W. Clark, J. D. Whittenberger. 1984. *Thermal Expansion of Binary CoAl, FeAl, and NiAl Alloys*. In: T. A. Hahn (ed.). *Thermal Expansion 8*. New York: Plenum Press.
- [35] Y. S. Touloukian, R. K. Kirby, R. E. Taylor, P. D. Desai. 1975. *Thermal Expansion: Metallic Elements and Alloys*. Thermophysical Properties of Matter: The TPRC Data Series, vol. 12. New York: Plenum.
- [36] Y. C. Zhou, T. Hashida. 2001. "Coupled Effects of Temperature Gradient and Oxidation on Thermal Stress in Thermal Barrier Coating System." *International Journal of Solids and Structures* 38(24–25): 4235–4264. DOI: 10.1016/S0020-7683(00)00309-7.
- [37] J. S. Eliseev, V. A. Poklad, O. G. Osipennikova, V. N. Larionov, A. V. Logunov, I. M. Razumovskij. 2008. *Composition of Heat-Resistant Nickel Alloy (Versions)*. Russia Patent: RU 2353691.
- [38] K. An, K. S. Ravichandran, R. E. Dutton, S. L. Semiatin. 1999. "Microstructure, Texture, and Thermal Conductivity of Single-Layer and Multilayer Thermal Barrier Coatings of  $Y_2O_3$ -Stabilized  $ZrO_2$  and  $Al_2O_3$  Made by Physical Vapor Deposition." *Journal of the American Ceramic Society* 82: 399–406. DOI: 10.1111/j.1551-2916.1999.tb20076.x.
- [39] B. T. F. Chung, M. M. Kermani, M. J. Braun, J. Padovan, R. C. Hendricks. 1985. "Heat Transfer in Thermal Barrier Coated Rods with Circumferential and Radial Temperature Gradients." *Journal of Engineering for Gas Turbines and Power* 107(1): 135–141. DOI: 10.1115/1.3239673.
- [40] D. Hasselman, L. F. Johnson, L. D. Bentzen, R. Syed, H. L. Lee, M. V. Swain. 1987. "Thermal Diffusivity and Conductivity of Dense Polycrystalline  $ZrO_2$  Ceramics: A Survey." *American Ceramic Society Bulletin* 66(5): 799–806.
- [41] J. C. Glandus, V. Tranchand. 1993. *Thermal Shock by Water Quench: Numerical Simulation*. In: G. A. Schneider, G. Petzow (eds). *Thermal Shock and Thermal Fatigue Behavior of Advanced Ceramics*. Dordrecht: Kluwer Academic Publishers.
- [42] M. Rohde. 1997. "Measuring and Modeling Thermal Conductivity in Thin Films and Microstructures." *High Temperatures – High Pressures* 29(2): 171–176.
- [43] R. E. Taylor. 1998. "Thermal Conductivity Determinations of Thermal Barrier Coatings." *Materials Science and Engineering: A* 245(2): 160–167.
- [44] X. Chen, J. Price, J. Ahmad. 2004. *Measuring and Modeling Residual Stresses in Air Plasma Spray Thermal Barrier Coatings*. In: E. Lara-Curcio, M. J. Readey. *28th International Conference on Advanced Ceramics and Composites*: B. Westerville, Ohio: The American Ceramic Society.
- [45] Y. Zhang, Y. Wang, K. Yin, H. Xu. 2004. "Finite Element Analysis of Residual Stresses in Zirconia Thermal Barrier Coatings on Superalloy." *Journal of the Ceramic Society of Japan*, Supplement 112: S1122–S1124. DOI: 10.14852/jcersjsuppl.112.0.S1122.0.
- [46] L. Wu, J. Zhu, H. Xie. 2014. "Numerical and Experimental Investigation of Residual Stress in Thermal Barrier Coatings during APS Process." *Journal of Thermal Spray Technology* 23: 653–665. DOI: 10.1007/s11666-014-0063-8.
- [47] Z. Gan, H. W. Ng, A. Devasenapathi. 2004. "Deposition-Induced Residual Stresses in Plasma-Sprayed Coatings." *Surface and Coatings Technology* 187(2–3): 307–319. DOI: 10.1016/j.surfcoat.2004.02.010.
- [48] M. Mohammadi, E. Poursaeidi. 2019. "Failure Mechanisms and Their Finite Element Modeling of Air Plasma Spray Thermal Barrier Coatings: A Review." *Advanced Materials and Novel Coatings* 7(27): 1937–1953. DOI: /amnc.2019.7.27.6.
- [49] G. Qian, T. Nakamura, C. C. Berndt. 1998. "Effects of Thermal Gradient and Residual Stresses on Thermal Barrier Coating Fracture." *Mechanics of Materials* 27(2): 91–110. DOI: 10.1016/S0167-6636(97)00042-2.
- [50] A. Bhattacharyya, D. Maurice. 2019. "Residual Stresses in Functionally Graded Thermal Barrier Coatings." *Mechanics of Materials* 129: 50–56. DOI: 10.1016/j.mechmat.2018.11.002.
- [51] W. G. Mao, Y. C. Zhou, L. Yang, X. H. Yu. 2006. "Modeling of Residual Stresses Variation with Thermal Cycling in Thermal Barrier Coatings." *Mechanics of Materials* 38(12): 1118–1127. DOI: 10.1016/j.mechmat.2006.01.002.
- [52] C. H. Hsueh, E. R. Fuller. 2000. "Analytical Modeling of Oxide Thickness Effects on Residual Stresses in Thermal Barrier Coatings." *Scripta Materialia* 42(8): 781–787. DOI: 10.1016/S1359-6462(99)00430-3.
- [53] S. Q. Nusier, G. M. Newaz. 1998. "Transient Residual Stresses in Thermal Barrier Coatings: Analytical and Numerical Results." *Journal of Applied Mechanics* 65(2): 346–353. DOI: 10.1115/1.2789061.
- [54] P. Bengtsson, C. Persson. 1997. "Modelled and Measured Residual Stresses in Plasma Sprayed Thermal Barrier Coatings." *Surface and Coatings Technology* 92(1–2): 78–86. DOI: 10.1016/S0257-8972(97)00082-0.
- [55] J. T. DeMasi, K. D. Sheffler, M. Ortiz. 1989. *Thermal Barrier Coating Life Prediction Model Development*. NASA Contractor Report 182230.
- [56] R. A. Miller. 1990. *Assessment of Fundamental Materials Needs for Thick Thermal Barrier Coatings (TTBC's) for Truck Diesel Engines*. NASA TM-103130: DOE/NASA/21794-1.
- [57] S. J. Schneider (ed.). 1991. *Engineering Materials Handbook: Ceramics and Glasses*. Almere: ASM International.
- [58] C. T. Sims, N. S. Stoloff, W. C. Hagel (eds). 1987. *Superalloys II: High-Temperature Materials for Aerospace and Industrial Power*. New York: John Wiley and Sons.
- [59] ASM Handbook Committee. 1990. *Properties and Selection: Irons, Steels, and High-Performance Alloys*. ASM International.
- [60] V. Teixeira, M. Andritschky, W. Fischer, H. P. Buchkremer, D. Stöver. 1999. "Effects of Deposition Temperature and Thermal Cycling on Residual Stress State in Zirconia-Based Thermal Barrier Coatings." *Surface and Coatings Technology* 120–121: 103–111. DOI: 10.1016/S0257-8972(99)00341-2.
- [61] H. Chen, Y. Liu, Y. Gao, S. Tao, H. Luo. 2010. "Design, Preparation, and Characterization of Graded  $YSZ/La_2Zr_2O_7$  Thermal Barrier Coatings." *Journal of the American Ceramic Society* 93: 1732–1740. DOI: 10.1111/j.1551-2916.2010.03610.x.
- [62] R. X. Hu, S. R. Liao, H. S. Zhang, Y. Wei. 2011. "Effect of Substrate Conditions on Residual Stress of Plasma-Spraying  $Sm_2Zr_2O_7$  Thermal Barrier Coatings." *Applied Mechanics and Materials* 84–85: 548–551. DOI: 10.4028/www.scientific.net/amm.84-85.548.
- [63] T. W. Clyne, S. C. Gill. 1996. "Residual Stresses in Thermal Spray Coatings and Their Effect on Interfacial Adhesion: A Review of Recent Work." *Journal of Thermal Spray Technology* 5: 401–418. DOI: 10.1007/BF02645271.
- [64] P. Skalka, K. Slámečka, J. Pokluda, L. Čelko. 2018. "Finite Element Simulation of Stresses in a Plasma-Sprayed Thermal Barrier Coating with a Crack at the TGO/Bond-Coat Interface." *Surface and Coatings Technology* 337: 321–334. DOI: 10.1016/j.surfcoat.2018.01.024.
- [65] H. Jahed, R. Shirazi. 2001. "Loading and Unloading Behaviour of a Thermoplastic Disc." *International Journal of Pressure Vessels and Piping* 78(9): 637–645. DOI: 10.1016/S0308-0161(01)00079-5.